INTERNATIONAL JOURNAL FOR NUMERICAL METHODS IN ENGINEERING
Int. J. Numer. Meth. Engng 2006; **67**:1318–1340
Published online 20 March 2006 in Wiley InterScience (www.interscience.wiley.com). DOI: 10.1002/nme.1665

A solution of the random eigenvalue problem by a dimensional decomposition method

Sharif Rahman*, †, ‡

Department of Mechanical and Industrial Engineering, The University of Iowa, Iowa City, IA 52242, U.S.A.

SUMMARY

This paper presents a dimensional decomposition method for obtaining probabilistic descriptors of real-valued eigenvalues of positive semi-definite random matrices. The method involves a novel function decomposition allowing lower-variate approximations of eigenvalues, lower-dimensional numerical integration for statistical moments, and Lagrange interpolation facilitating efficient Monte Carlo simulation for probability density functions. Compared with commonly-used perturbation and recently-developed asymptotic methods, no derivatives of eigenvalues are required by the new method developed. Results of numerical examples from structural dynamics indicate that the decomposition method provides excellent estimates of moments and probability densities of eigenvalues for various cases including closely-spaced modes and large statistical variations of input. Copyright © 2006 John Wiley & Sons, Ltd.

KEY WORDS: random eigenvalue; random matrix theory; decomposition method; univariate decomposition; bivariate decomposition; moment of eigenvalue; probability density of eigenvalue

1. INTRODUCTION

Random matrix theory is concerned with determining probabilistic characteristics of eigenvalues and eigenvectors of matrices defined by a statistical distribution. Since first introduced by Wishart [1] in 1928, random matrices have fascinated both mathematicians and physicists with far-reaching applications in many different areas. However, it was not until the early 1950s when the subject gained prominence with Wigner's pioneering work in nuclear physics [2]. The mathematical foundation of the theory was later established in a series of landmark papers by Wigner [3], Mehta [4], and Dyson [5]. An excellent exposition of the random matrix theory

*Correspondence to: Sharif Rahman, Department of Mechanical and Industrial Engineering, The University of Iowa, Iowa City, IA 52242, U.S.A.
†E-mail: rahman@engineering.uiowa.edu, http://www.engineering.uiowa.edu/∼rahman
‡Professor.

Contract/grant sponsor: U.S. National Science Foundation; contract/grant number: DMI-0355487

Received 14 September 2005
Revised 13 January 2006
Accepted 13 January 2006

can be found in Mehta's seminal work [6]. Nowadays, random matrices find applications in fields as diverse as quantum physics, number theory, multivariate statistics, graph theory, signal processing and communication, finance, computational biology, and of course, mechanics.

In random matrix theory much attention has been given to three important Gaussian (also known as Hermite) ensembles: *orthogonal*, *unitary*, and *symplectic* [6, 7]. If an $L \times L$ random matrix $\mathbf{G}$, comprising of independent and identically distributed standard Gaussian elements $[G_{ij}]$, defines a Gaussian random matrix, then the symmetric $L \times L$ random matrix $(\mathbf{G}+\mathbf{G}^{\mathrm{T}})/2$ is called the Gaussian orthogonal ensemble. There are complex and quaternion analogs of the Gaussian orthogonal ensemble and are known as Gaussian unitary ensemble and Gaussian symplectic ensemble, respectively. For all three Gaussian ensembles, the joint probability density of eigenvalues can be derived exactly [6]. Closed-form solutions also exist for other classical ensembles associated with the Wishart (or Laguerre) and the multivariate analysis of variance (or Jacobi) random matrices [7]. While these analytical solutions provide significant insight, random matrices encountered in engineering unfortunately do not follow specific matrix structures or probability distributions of classical ensembles. Therefore, approximate methods involving sound theoretical foundation and advanced computational techniques are required to solve a general random eigenvalue problem.

In engineering, random matrices frequently appear in structural dynamics and structural stability, among others. The evaluation of modal frequencies and buckling of mechanical systems involves solution of eigenvalue problems for stochastic differential operators and matrices. The randomness in these operators or matrices comes from the statistical variability of material parameters (e.g. mass, damping, stiffness) and geometry (e.g. size, shape, topology), and constraints (e.g. boundary conditions). Current approximate methods for solving random eigenvalue problems include the Taylor series or perturbation method [8–10], the iteration method [8], the Ritz method [11], the crossing theory [12], the stochastic reduced basis [13], the subspace iteration [14], and the asymptotic method [15]. Among these methods, perturbation methods have dominated the current literature. These methods involve first- or second-order Taylor series expansions of the eigenvalue or eigenvector in terms of basic input random parameters and application of standard stochastic operators to obtain second-moment properties of output. Two major limitations of these methods are that both the uncertainty of random input and the non-linearity of random eigenvalue or eigenvector with respect to random input must be small. The errors in these methods can be bounded if higher-order partial derivatives of the eigenvalue or eigenvector variable exist and are available. However, such bounds are rarely used in engineering applications since they require expensive calculations of higher-order partial derivatives. The direct Monte Carlo simulation can be applied to solve any random eigenvalue problem. However, it usually is prohibitive when dealing with large matrices. Consequently, the simulation method is useful only when alternative methods are inapplicable or inaccurate, and has been traditionally employed as a yardstick for evaluating approximate methods.

This paper presents a new decomposition method for predicting statistical moments and probability density functions of eigenvalues of real, positive semi-definite, stochastic matrices. Section 2 formally defines the random eigenvalue problem involving matrix operators. Section 3 gives a brief exposition of a novel function decomposition that facilitates lower-dimensional approximations of eigenvalues. Section 4 describes the proposed decomposition method and associated computational effort for calculating statistical moments and probability density functions of eigenvalues. Three numerical examples from structural dynamics illustrate the method developed in Section 5. Comparisons have been made with alternative approximate and

simulation methods to evaluate the accuracy and computational efficiency of the new method. Finally, Section 6 provides conclusions and outlook from this work.

2. RANDOM EIGENVALUE PROBLEM

Let $(\Omega, \mathscr{F}, P)$ be a probability space, where Ω is the sample space, $\mathscr{F}$ is the σ-algebra of subsets of Ω, and P is the probability measure; $\mathbb{R}^N$ be an N-dimensional real vector space; and $\mathbb{M}_L^{S+0}(\mathbb{R})$ be a set of all $L \times L$, real-valued, symmetric, positive semi-definite matrices. Defined on the probability space endowed with the expectation operator $\mathbb{E}$, consider a real-valued N-dimensional random vector $\mathbf{X} = \{X_1, \ldots, X_N\}^{\mathrm{T}} \in \mathbb{R}^N$ with mean vector $\boldsymbol{\mu}_{\mathbf{X}} \equiv \mathbb{E}[\mathbf{X}] \in \mathbb{R}^N$, covariance matrix $\boldsymbol{\Sigma}_{\mathbf{X}} \equiv \mathbb{E}[(\mathbf{X} - \boldsymbol{\mu}_{\mathbf{X}})(\mathbf{X} - \boldsymbol{\mu}_{\mathbf{X}})^{\mathrm{T}}] \in \mathbb{M}_N^{S+0}(\mathbb{R})$, and joint probability density function $f_{\mathbf{X}}(\mathbf{x}) : \mathbb{R}^N \mapsto \mathbb{R}$. For undamped or proportionally damped systems, let $\mathbf{K}(\mathbf{X}) \in \mathbb{M}_L^{S+0}(\mathbb{R})$ and $\mathbf{M}(\mathbf{X}) \in \mathbb{M}_L^{S+0}(\mathbb{R})$ denote $L \times L$, real-valued, symmetric, positive semi-definite, random stiffness and random mass matrices, respectively, where elements $[K_{ij}(\mathbf{X}) : \mathbb{R}^N \mapsto \mathbb{R}]$ and $[M_{ij}(\mathbf{X}) : \mathbb{R}^N \mapsto \mathbb{R}]$; $i, j = 1, \ldots, L$. The probabilistic characteristics of random matrices $\mathbf{K}(\mathbf{X})$ and $\mathbf{M}(\mathbf{X})$ can be derived from the probability law of $\mathbf{X}$.

The generalized linear random eigenvalue problem for a random matrix pair $\{\mathbf{K}(\mathbf{X}), \mathbf{M}(\mathbf{X})\}$ is defined as

$$\mathbf{K}(\mathbf{X})\boldsymbol{\Phi}(\mathbf{X}) = \Lambda(\mathbf{X})\mathbf{M}(\mathbf{X})\boldsymbol{\Phi}(\mathbf{X}) \tag{1}$$

where $\{\Lambda^{(i)}(\mathbf{X}), \boldsymbol{\Phi}^{(i)}(\mathbf{X})\}$, $i = 1, \ldots, L$ is the ith eigenpair that includes random eigenvalue $\Lambda^{(i)}(\mathbf{X})$ and random eigenvector $\boldsymbol{\Phi}^{(i)}(\mathbf{X})$. Based on the properties of $\mathbf{K}(\mathbf{X})$ and $\mathbf{M}(\mathbf{X})$, Equation (1) yields real and non-negative eigenvalues $\{\Lambda^{(i)}(\mathbf{X})\}$, $i = 1, \ldots, L$ with probability one, where $\Lambda(\mathbf{X})$ depends on random input $\mathbf{X}$ via solution of the matrix characteristic equation

$$\det[\mathbf{K}(\mathbf{X}) - \Lambda(\mathbf{X})\mathbf{M}(\mathbf{X})] = 0 \tag{2}$$

A major objective in solving a random eigenvalue problem is to find probabilistic characteristics of eigenpair $\{\Lambda^{(i)}(\mathbf{X}), \boldsymbol{\Phi}^{(i)}(\mathbf{X})\}$ when the probability law of $\mathbf{X}$ is arbitrarily prescribed.

The direct Monte Carlo simulation can be applied to solve any random eigenvalue problem. It involves: (1) generating samples $\mathbf{k}(\mathbf{x}_k)$ and $\mathbf{m}(\mathbf{x}_k)$; $k = 1, \ldots, K$ from K input samples $\mathbf{x}_k$; $k = 1, \ldots, K$; (2) solving the corresponding characteristic equation $\det[\mathbf{k}(\mathbf{x}_k) - \lambda(\mathbf{x}_k)\mathbf{m}(\mathbf{x}_k)] = 0$ to find samples of eigenpairs $\{\lambda_k^{(i)}, \boldsymbol{\phi}_k^{(i)}\}$; $i = 1, \ldots, L$; $k = 1, \ldots, K$; and (3) developing statistics of $\{\Lambda^{(i)}, \boldsymbol{\Phi}^{(i)}\}$; $i = 1, \ldots, L$ from $\{\lambda_k^{(i)}, \boldsymbol{\phi}_k^{(i)}\}$; $i = 1, \ldots, L$; $k = 1, \ldots, K$. The direct simulation can provide full probabilistic description of the eigenvalues and eigenvectors of $\{\mathbf{K}(\mathbf{X}), \mathbf{M}(\mathbf{X})\}$, but it is computationally inefficient when $\mathbf{K}(\mathbf{X})$ and $\mathbf{M}(\mathbf{X})$ are large because it requires solving the matrix characteristic equation for every realization of $\mathbf{K}(\mathbf{X})$ and $\mathbf{M}(\mathbf{X})$.

3. GENERAL EIGENVALUE DECOMPOSITION

Consider a continuous, differentiable, real-valued eigenvalue $\lambda(\mathbf{x}) : \mathbb{R}^N \mapsto \mathbb{R}$ that depends on $\mathbf{x} = \{x_1, \ldots, x_N\}^{\mathrm{T}} \in \mathbb{R}^N$. A dimensional decomposition of a general multivariate function $\lambda(\mathbf{x})$,

described by [16, 17]

$$\lambda(\mathbf{x}) = \underbrace{\underbrace{\lambda_0 + \sum_{i=1}^{N} \lambda_i(x_i)}_{=\hat{\lambda}_1(\mathbf{x})} + \sum_{\substack{i_1,i_2=1 \\ i_1<i_2}}^{N} \lambda_{i_1 i_2}(x_{i_1}, x_{i_2})}_{=\hat{\lambda}_2(\mathbf{x})} + \cdots + \underbrace{\sum_{\substack{i_1,\ldots,i_S=1 \\ i_1<\cdots<i_S}}^{N} \lambda_{i_1\cdots i_S}(x_{i_1}, \ldots, x_{i_s}) + \cdots + \lambda_{12\cdots N}(x_1, \ldots, x_N)}_{=\hat{\lambda}_S(\mathbf{x})} \tag{3}$$

can be viewed as a finite hierarchical expansion of an output function in terms of its input variables with increasing dimension, where λ_0 is a constant, $\lambda_i(x_i) : \mathbb{R} \mapsto \mathbb{R}$ is a univariate component function representing individual contribution to $\lambda(\mathbf{x})$ by input variable x_i acting alone, $\lambda_{i_1 i_2}(x_{i_1}, x_{i_2}) : \mathbb{R}^2 \mapsto \mathbb{R}$ is a bivariate component function describing cooperative influence of two input variables x_{i_1} and x_{i_2}, $\lambda_{i_1\cdots i_S}(x_{i_1}, \ldots, x_{i_S}) : \mathbb{R}^S \mapsto \mathbb{R}$ is an S-variate component function quantifying cooperative effects of S input variables $x_{i_1}, \ldots, x_{i_S}$, and so on. The individual contribution does not imply that input variables, if random, are required to be statistically uncorrelated or independent. If

$$\hat{\lambda}_S(\mathbf{x}) = \lambda_0 + \sum_{i=1}^{N} \lambda_i(x_i) + \sum_{\substack{i_1,i_2=1 \\ i_1<i_2}}^{N} \lambda_{i_1 i_2}(x_{i_1}, x_{i_2}) + \cdots + \sum_{\substack{i_1,\ldots,i_S=1 \\ i_1<\cdots<i_S}}^{N} \lambda_{i_1\cdots i_S}(x_{i_1}, \ldots, x_{i_s}) \tag{4}$$

represents a general S-variate approximation of $\lambda(\mathbf{x})$, the univariate ($S=1$) and bivariate ($S=2$) approximations $\hat{\lambda}_1(\mathbf{x})$ and $\hat{\lambda}_2(\mathbf{x})$, respectively, provide two- and three-term approximants of the finite decomposition in Equation (3). Similarly, trivariate, quadrivariate, and other higher-variate approximations can be derived by appropriately selecting the value of S. The fundamental conjecture underlying this work is that component functions arising in the eigenvalue function decomposition will exhibit insignificant S-variate effects cooperatively when $S \to N$, leading to useful lower-variate approximations of $\lambda(\mathbf{x})$. In the limit, when $S=N$, $\hat{\lambda}_S(\mathbf{x})$ converges to the exact function $\lambda(\mathbf{x})$. In other words, Equation (4) generates a hierarchical and convergent sequence of approximations of $\lambda(\mathbf{x})$.

4. DIMENSIONAL DECOMPOSITION METHOD

4.1. Lower-variate approximations of eigenvalues

Consider univariate and bivariate approximations of $\lambda(\mathbf{x})$, respectively, defined by

$$\hat{\lambda}_1(\mathbf{x}) \equiv \hat{\lambda}_1(x_1, \ldots, x_N) \equiv \sum_{i=1}^{N} \underbrace{\lambda(c_1, \ldots, c_{i-1}, x_i, c_{i+1}, \ldots, c_N)}_{=\lambda_i(x_i)} \underbrace{-(N-1)\lambda(\mathbf{c})}_{=\lambda_0} \tag{5}$$

$$\hat{\lambda}_2(\mathbf{x}) \equiv \hat{\lambda}_2(x_1, \ldots, x_N) \equiv \sum_{\substack{i_1,i_2=1 \\ i_1<i_2}}^{N} \overbrace{\lambda(c_1, \ldots, c_{i_1-1}, x_{i_1}, c_{i_1+1}, \ldots, c_{i_2-1}, x_{i_2}, c_{i_2+1}, \ldots, c_N)}^{=\lambda_{i_1 i_2}(x_{i_1}, x_{i_2})}$$

$$+\sum_{i=1}^{N}\underbrace{-(N-2)\lambda(c_1,\ldots,c_{i-1},x_i,c_{i+1},\ldots,c_N)}_{=\lambda_i(x_i)}$$

$$+\underbrace{\frac{(N-1)(N-2)}{2}\lambda(\mathbf{c})}_{=\lambda_0} \tag{6}$$

where $\mathbf{c}=\{c_1,\ldots,c_N\}^{\mathrm{T}}$ is a reference point in the input domain, $\lambda(\mathbf{c})\equiv\lambda(c_1,\ldots,c_N)$, $\lambda_i(x_i)\equiv\lambda(c_1,\ldots,c_{i-1},x_i,c_{i+1},\ldots,c_N)$, $\lambda_{i_1i_2}(x_{i_1},x_{i_2})\equiv\lambda(c_1,\ldots,c_{i_1-1},x_{i_1},c_{i_1+1},\ldots,c_{i_2-1},x_{i_2},c_{i_2+1},\ldots,c_N)$. Based on the author's past experience, the mean point of random input defines a suitable reference point. Nevertheless, these two approximations of $\lambda(\mathbf{x})$ can be generalized to an S-variate approximation for any integer $1\leqslant S\leqslant N$, given by

$$\hat{\lambda}_S(\mathbf{x})\equiv\sum_{i=0}^{S}(-1)^i\binom{N-S+i-1}{i}$$

$$\times\sum_{\substack{k_1,\ldots,k_{S-i}=1\\ k_1<\cdots<k_{S-i}}}^{N}\lambda(c_1,\ldots,c_{k_1-1},x_{k_1},c_{k_1+1},\ldots,c_{k_{S-i}-1},x_{k_{S-i}},c_{k_{S-i}+1},\ldots,c_N) \tag{7}$$

where $\lambda(c_1,\ldots,c_{k_1-1},x_{k_1},c_{k_1+1},\ldots,c_{k_{S-i}-1},x_{k_{S-i}},c_{k_{S-i}+1},\ldots,c_N)$ is an $(S-i)$th dimensional component function representing $(S-i)$th dimensional cooperation among input variables $x_{k_1},\ldots,x_{k_{S-i}}$. Using a multivariate function theorem developed by Xu and Rahman [18], it can be shown that $\hat{\lambda}_S(\mathbf{x})$ in Equation (7) consists of all terms of the Taylor series of $\lambda(\mathbf{x})$ that have less than or equal to S variables. The expanded form of Equation (7), when compared with the Taylor expansion of $\lambda(\mathbf{x})$, indicates that the residual error in the S-variate approximation is $\lambda(\mathbf{x})-\hat{\lambda}_S(\mathbf{x})=\mathscr{R}_{S+1}$, where the remainder $\mathscr{R}_{S+1}$ includes terms of dimensions $S+1$ and higher. When $S=1$ and 2, Equation (7) degenerates to univariate (Equation (5)) and bivariate (Equation (6)) approximations, respectively.

It is worth noting that the univariate or bivariate approximations should not viewed as first- or second-order Taylor series expansions nor do they limit the non-linearity of $\lambda(\mathbf{x})$. In fact, all higher-order univariate or bivariate terms of $\lambda(\mathbf{x})$ are included in Equations (5) or (6), which should therefore provide in general higher-order representation of eigenvalues than those by commonly employed first- or second-order perturbation methods.

4.2. Statistical moments of eigenvalues

The lth statistical moment of a random eigenvalue $\Lambda(\mathbf{X})$ is defined as

$$m_l\equiv\mathbb{E}[\Lambda^l(\mathbf{X})]=\int_{\mathbb{R}^N}\lambda^l(\mathbf{x})\,f_{\mathbf{X}}(\mathbf{x})\,\mathrm{d}\mathbf{x} \tag{8}$$

In reference to Equations (5)–(7), the univariate, bivariate, and generalized S-variate approximations of $\Lambda^l(\mathbf{X})$ yield

$$m_l \cong \mathbb{E}[\hat{\Lambda}_1^l(\mathbf{X})] = \sum_{i=1}^{N} \mathbb{E}[\Lambda^l(c_1, \ldots, c_{i-1}, X_i, c_{i+1}, \ldots, c_N)] - (N-1)\lambda^l(\mathbf{c}) \tag{9}$$

$$\begin{aligned} m_l \cong \mathbb{E}[\hat{\Lambda}_2^l(\mathbf{X})] = \mathbb{E}&\left[\sum_{\substack{i_1,i_2=1 \\ i_1<i_2}}^{N} \Lambda^l(c_1, \ldots, c_{i_1-1}, X_{i_1}, c_{i_1+1}, \ldots, c_{i_2-1}, X_{i_2}, c_{i_2+1}, \ldots, c_N)\right] \\ &- (N-2)\mathbb{E}\left[\sum_{i=1}^{N} \Lambda^l(c_1, \ldots, c_{i-1}, X_i, c_{i+1}, \ldots, c_N)\right] \\ &+ \frac{(N-1)(N-2)}{2}\lambda^l(\mathbf{c}) \end{aligned} \tag{10}$$

and

$$\begin{aligned} m_l \cong \mathbb{E}[\hat{\Lambda}_S^l(\mathbf{X})] = &\sum_{i=0}^{S} (-1)^i \binom{N-S+i-1}{i} \\ &\times \mathbb{E}\left[\sum_{\substack{k_1,\ldots,k_{S-i}=1 \\ k_1<\cdots<k_{S-i}}}^{N} \Lambda^l(c_1, \ldots, c_{k_1-1}, X_{k_1}, c_{k_1+1}, \ldots, c_{k_{S-i}-1}, X_{k_{S-i}}, c_{k_{S-i}+1}, \ldots, c_N)\right] \end{aligned} \tag{11}$$

respectively. As with Equation (4), the expectation $\mathbb{E}[\hat{\Lambda}_S^l(\mathbf{X})]$ for $S = 1, 2, \ldots, N$ also represents a hierarchical and convergent sequence of approximations of the lth moment of an eigenvalue. Note that only one-, at most two-, and at most S-dimensional deterministic integrations are involved in evaluating the expectations in Equations (9), (10), and (11), respectively. For independent random vector $\mathbf{X}$, the S-variate approximation of moments can be easily evaluated using standard numerical quadratures, leading to

$$\begin{aligned} m_l \cong \mathbb{E}[\hat{\Lambda}_S^l(\mathbf{X})] \cong &\sum_{i=0}^{S} (-1)^i \binom{N-S+i-1}{i} \sum_{\substack{k_1,\ldots,k_{S-i}=1 \\ k_1<\cdots<k_{S-i}}}^{N} \sum_{j_{S-i}=1}^{n} \cdots \sum_{j_1=1}^{n} w_{k_1}^{(j_1)} \cdots w_{k_{S-i}}^{(j_{S-i})} \\ &\times \lambda^l(c_1, \ldots, c_{k_1-1}, x_{k_1}^{(j_1)}, c_{k_1+1}, \ldots, c_{k_{S-i}-1}, x_{k_{S-i}}^{(j_{S-i})}, c_{k_{S-i}+1}, \ldots, c_N) \end{aligned} \tag{12}$$

where $x_i^{(j)}$ is the jth integration point of the ith variable, $w_i^{(j)}$ is the associated weight, and n is the order of integration. For example, Gauss–Legendre or Gauss–Hermite quadratures are frequently used when X_i follows uniform or Gaussian distributions, respectively. For an arbitrary distribution, X_i can be transformed to a uniform or Gaussian variable, followed

by Gauss–Legendre or Gauss–Hermite quadratures. If $\mathbf{X}$ consists of dependent variables, an appropriate transformation, such as the Rosenblatt transformation [19], should be applied to map the dependent random vector to an independent standard Gaussian random vector. Similar approximations can be developed for obtaining moments of any functions of eigenvalues or joint moments (e.g. correlation coefficients) of eigenvalues if desired.

The method for solving moments of eigenvalues employing Equations (9) or (10) and numerical integrations are defined as the *univariate* or *bivariate decomposition method* in this paper. The method developed does not require calculation of any partial derivatives of eigenvalues as compared with the perturbation or asymptotic methods.

4.3. Probability density functions of eigenvalues

4.3.1. Lagrange interpolation. Consider the univariate component function $\lambda_i(x_i) \equiv \lambda(c_1, \ldots, c_{i-1}, x_i, c_{i+1}, \ldots, c_N)$ in Equation (5) or (6). If for sample points $x_i = x_i^{(j)}$; $j = 1, \ldots, n$, n distinct eigenvalues $\lambda(c_1, \ldots, c_{i-1}, x_i^{(j)}, c_{i+1}, \ldots, c_N)$; $j = 1, \ldots, n$ are given, the eigenvalue for an arbitrary x_i can be obtained by the Lagrange interpolation[§]

$$\lambda_i(x_i) = \sum_{j=1}^{n} \phi_j(x_i) \lambda(c_1, \ldots, c_{i-1}, x_i^{(j)}, c_{i+1}, \ldots, c_N) \tag{13}$$

where

$$\phi_j(x_i) = \frac{\prod_{k=1, k\neq j}^{n} (x_i - x_i^{(k)})}{\prod_{k=1, k\neq j}^{n} (x_i^{(j)} - x_i^{(k)})} \tag{14}$$

is the shape function. By using Equations (13) and (14), arbitrarily many values of $\lambda_i(x_i)$ can be generated if n values of that component function are given. The same idea can be applied to the bivariate component function $\lambda_{i_1 i_2}(x_{i_1}, x_{i_2}) \equiv \lambda(c_1, \ldots, c_{i_1-1}, x_{i_1}, c_{i_1+1}, \ldots, c_{i_2-1}, x_{i_2}, c_{i_2+1}, \ldots, c_N)$ in Equation (6). If for $x_{i_1} = x_{i_1}^{(j_1)}$ and $x_{i_2} = x_{i_2}^{(j_2)}$, n^2 function values $\lambda_{i_1 i_2}(x_{i_1}^{(j_1)}, x_{i_2}^{(j_2)}) \equiv \lambda(c_1, \ldots, c_{i_1-1}, x_{i_1}^{(j_1)}, c_{i_1+1}, \ldots, c_{i_2-1}, x_{i_2}^{(j_2)}, c_{i_2+1}, \ldots, c_N)$; $j_1, j_2 = 1, \ldots, n$ are given, the function value for an arbitrary point (x_{i_1}, x_{i_2}) can be obtained using the Lagrange interpolation

$$\lambda_{i_1 i_2}(x_{i_1}, x_{i_2}) = \sum_{j_2=1}^{n} \sum_{j_1=1}^{n} \phi_{j_1}(x_{i_1}) \phi_{j_2}(x_{i_2}) \lambda(c_1, \ldots, c_{i_1-1}, x_{i_1}^{(j_1)}$$

$$c_{i_1+1}, \ldots, c_{i_2-1}, x_{i_2}^{(j_2)}, c_{i_2+1}, \ldots, c_N) \tag{15}$$

The same procedure is repeated for all univariate and bivariate component functions, i.e. for all $\lambda_i(x_i), i = 1, \ldots, N$ and for all $\lambda_{i_1 i_2}(x_{i_1}, x_{i_2}), i_1, i_2 = 1, \ldots, N$, leading to the univariate

[§]In general, integer n symbolizes the number of points at a given co-ordinate where deterministic eigenvalue analyses are performed. It represents either the *number of sample points* required for evaluating probability density or the *integration order* required for statistical moment analysis.

approximation

$$\hat{\Lambda}_1(\mathbf{X}) \cong \sum_{i=1}^{N} \sum_{j=1}^{n} \phi_j(X_i)\lambda(c_1, \ldots, c_{i-1}, x_i^{(j)}, c_{i+1}, \ldots, c_N) - (N-1)\lambda(\mathbf{c}) \tag{16}$$

and to the bivariate approximation

$$\hat{\Lambda}_2(\mathbf{X}) \equiv \sum_{\substack{i_1, i_2=1 \\ i_1<i_2}}^{N} \sum_{j_2=1}^{n} \sum_{j_1=1}^{n} \phi_{j_1}(X_{i_1})\phi_{j_2}(X_{i_2})\lambda(c_1, \ldots, c_{i_1-1}, x_{i_1}^{(j_1)}, c_{i_1+1}, \ldots, c_{i_2-1}, x_{i_2}^{(j_2)}$$

$$c_{i_2+1}, \ldots, c_N) - (N-2)\sum_{i=1}^{N} \sum_{j=1}^{n} \phi_j(X_i)\lambda(c_1, \ldots, c_{i-1}, x_i^{(j)}$$

$$c_{i+1}, \ldots, c_N) + \frac{(N-1)(N-2)}{2}\lambda(\mathbf{c}) \tag{17}$$

Following a similar consideration, the generalized S-variate approximation can be derived as

$$\hat{\Lambda}_S(\mathbf{X}) = \sum_{i=0}^{S} (-1)^i \binom{N-S+i-1}{i} \sum_{\substack{k_1, \ldots, k_{S-i}=1 \\ k_1<\cdots<k_{S-i}}}^{N} \sum_{j_{S-i}=1}^{n} \cdots \sum_{j_1=1}^{n} \phi_{j_1}(X_{k_1}) \cdots \phi_{j_{S-i}}(X_{k_{S-i}})$$

$$\times \lambda(c_1, \ldots, c_{k_1-1}, x_{k_1}^{(j_1)}, c_{k_1+1}, \ldots, c_{k_{S-i}-1}, x_{k_{S-i}}^{(j_{S-i})}, c_{k_{S-i}+1}, \ldots, c_N) \tag{18}$$

which can be utilized to generate higher-variate approximations if desired. But, due to their higher cost, only univariate and bivariate approximations are considered in this paper. Nevertheless, Equation (18) provides a convergent sequence of lower-variate approximations of $\Lambda(\mathbf{X})$.

4.3.2. Monte Carlo simulation. Once the Lagrange shape functions $\phi_j(x_i)$ and deterministic coefficients $\lambda(\mathbf{c})$, $\lambda(c_1, \ldots, c_{i-1}, x_i^{(j)}, c_{i+1}, \ldots, c_N)$, $\lambda(c_1, \ldots, c_{i_1-1}, x_{i_1}^{(j_1)}, c_{i_1+1}, \ldots, c_{i_2-1}, x_{i_2}^{(j_2)}$, $c_{i_2+1}, \ldots, c_N)$, and $\lambda(c_1, \ldots, c_{k_1-1}, x_{k_1}^{(j_1)}, c_{k_1+1}, \ldots, c_{k_{S-i}-1}, x_{k_{S-i}}^{(j_{S-i})}, c_{k_{S-i}+1}, \ldots, c_N)$ are generated, Equations (16)–(18) provide explicit approximations of random eigenvalues $\{\Lambda^{(i)}(\mathbf{X})\}$, $i = 1, \ldots, L$ in terms of random input $\mathbf{X}$. Therefore, any probabilistic characteristics of eigenvalues, including the marginal or the joint probability density function of $\{\Lambda^{(i)}(\mathbf{X})\}$, $i = 1, \ldots, L$, can be easily evaluated by performing Monte Carlo simulation on Equations (16)–(18). Since Equations (16)–(18) do not require solving additional matrix equations, the embedded Monte Carlo simulation can be efficiently conducted for any sample size. It is worth noting that moments of eigenvalues can also be determined from samples generated using Equations (16)–(18).

The proposed method involving univariate (Equation (16)) or bivariate (Equation (17)) approximations, n-point Lagrange interpolation (Equations (13)–(15)), and associated Monte Carlo simulation are also defined as the *univariate* or *bivariate decomposition method* in this paper. Again, no partial derivatives of eigenvalues are required.

4.4. Computational effort

The univariate and bivariate approximations employed in calculating both moments and probability density functions of eigenvalues require evaluation of $\lambda(\mathbf{c})$, $\lambda(c_1, \ldots, c_{i-1}, x_i^{(j)}, c_{i+1}, \ldots, c_N)$, and $\lambda(c_1, \ldots, c_{i_1-1}, x_{i_1}^{(j_1)}, c_{i_1+1}, \ldots, c_{i_2-1}, x_{i_2}^{(j_2)}, c_{i_2+1}, \ldots, c_N)$ for $i, i_1, i_2 = 1, \ldots, N$ and j, $j_1, j_2 = 1, \ldots, n$. Hence, the computational effort required by the proposed method can be viewed as numerically solving the associated deterministic characteristic equations

$$\det[\mathbf{k}(\mathbf{c}) - \lambda(\mathbf{c})\mathbf{m}(\mathbf{c})] = 0 \tag{19}$$

$$\begin{aligned}\det[&\mathbf{k}(c_1, \ldots, c_{i-1}, x_i^{(j)}, c_{i+1}, \ldots, c_N) - \lambda(c_1, \ldots, c_{i-1}, x_i^{(j)}, c_{i+1}, \ldots, c_N)\\ &\times \mathbf{m}(c_1, \ldots, c_{i-1}, x_i^{(j)}, c_{i+1}, \ldots, c_N)] = 0; \quad i = 1, \ldots, N; \quad j = 1, \ldots, n\end{aligned} \tag{20}$$

and

$$\begin{aligned}\det[&\mathbf{k}(c_1, \ldots, c_{i_1-1}, x_{i_1}^{(j_1)}, c_{i_1+1}, \ldots, c_{i_2-1}, x_{i_2}^{(j_2)}, c_{i_2+1}, \ldots, c_N)\\ &- \lambda(c_1, \ldots, c_{i_1-1}, x_{i_1}^{(j_1)}, c_{i_1+1}, \ldots, c_{i_2-1}, x_{i_2}^{(j_2)}, c_{i_2+1}, \ldots, c_N)\\ &\times \mathbf{m}(c_1, \ldots, c_{i_1-1}, x_{i_1}^{(j_1)}, c_{i_1+1}, \ldots, c_{i_2-1}, x_{i_2}^{(j_2)}, c_{i_2+1}, \ldots, c_N)] = 0\\ &i_1, i_2 = 1, \ldots, N; \quad j_1, j_2 = 1, \ldots, n\end{aligned} \tag{21}$$

at several deterministic input defined by either integration points (moments) or user-selected sample points (probability density functions). There are n and n^2 numerical evaluations of $\lambda(\mathbf{x})$ involved in Equations (13) and (15), respectively. Therefore, the total cost for the univariate method entails a *maximum* of $nN + 1$ solutions of the matrix characteristic equation; and a *maximum* of $N(N-1)n^2/2 + nN + 1$ solutions of the matrix characteristic equation are required for the bivariate method. If the integration or sample points include a common point in each co-ordinate x_i (see the Example section), the numbers of such solutions reduces to $(n-1)N+1$ and $N(N-1)(n-1)^2/2 + (n-1)N + 1$ for univariate and bivariate methods, respectively.

The dimensional decomposition presented in this paper can be extended to evaluate stochastic characteristics of eigenvectors. For example, the decomposition of a scalar function in Equation (3) can also be employed to express an eigenvector as a finite sum of component vectors, which are functions of input variables with increasing dimension. The probabilistic characterization of eigenvectors and their use in stochastic dynamics are subjects of future work.

5. NUMERICAL EXAMPLES

Three numerical examples involving linear dynamics of spring-mass systems and a cantilever plate are presented to illustrate the decomposition method. Whenever possible, comparisons have been made with commonly-used mean-centred perturbation methods, a recently developed asymptotic method, and the direct Monte Carlo simulation to evaluate the accuracy and efficiency of the proposed method. The Gaussian assumption of random input in Example 1 was adopted mainly for comparing the decomposition method with existing methods that employ Gaussian input with readily available results. The method developed does not require the Gaussian assumption, as illustrated in Examples 2 and 3. For the first two examples, the eigenvalues were calculated by an IMSL subroutine, which employs a hybrid double-shifted LR-QR algorithm [20]. A Lanczos algorithm embedded in the finite element code ABAQUS (Version 6.5) [21] was employed to obtain eigenvalues for the third example.

In all three examples, the univariate and/or bivariate decompositions were formulated in the Gaussian image (**u** space) of the original space (**x** space) of random input. The reference point **c** associated with the decomposition method was fixed at the mean input in the **u** space. For moment analysis, a 5th-order (i.e. $n=5$) Gauss–Hermite integration was employed in obtaining the tabulated results of Example 1. In Examples 2 and 3, which involve calculation of probability densities of eigenvalues, 5 (i.e. $n=5$) sample points $(c_1, \ldots, c_{i-1}, u_i^{(j)}, c_{i+1}, \ldots, c_N)$ and $(c_1, \ldots, c_{i_1-1}, u_{i_1}^{(j_1)}, c_{i_1+1}, \ldots, c_{i_2-1}, u_{i_2}^{(j_2)}, c_{i_2+1}, \ldots, c_N)$ in the **u** space were chosen with $c_i=0$ and uniformly distributed points $u_i^{(j)}$ or $u_{i_1}^{(j_1)}$ or $u_{i_2}^{(j_2)}=-2,-1,0,1,2$. For both moment and probability density analyses, $(n-1)N+1$ and $(n-1)^2N(N-1)/2+(n-1)N+1$ solutions of the matrix characteristic equation are involved in univariate and bivariate methods, respectively, in all three examples.

5.1. Example 1—a two-degree-of-freedom undamped spring-mass system

As shown in Figure 1, consider a two-degree-of-freedom undamped spring-mass system with a deterministic mass matrix

$$\mathbf{m}=\begin{bmatrix} m_1 & 0 \\ 0 & m_2 \end{bmatrix} \in \mathbb{M}_2^{S+0}(\mathbb{R}) \tag{22}$$

and a random stiffness matrix

$$\mathbf{K}(\mathbf{X})=\begin{bmatrix} K_1(\mathbf{X})+k_3 & -k_3 \\ -k_3 & K_2(\mathbf{X})+k_3 \end{bmatrix} \in \mathbb{M}_2^{S+0}(\mathbb{R}) \tag{23}$$

where masses $m_1=1\,\text{kg}$, $m_2=1.5\,\text{kg}$, and spring stiffnesses $K_1(\mathbf{X})=1000(1+0.25X_1)\,\text{N/m}$, $K_2(\mathbf{X})=1100(1+0.25X_2)\,\text{N/m}$, and $k_3=100\,\text{N/m}$ [15]. The input $\mathbf{X}=\{X_1, X_2\}^{\mathrm{T}} \in \mathbb{R}^2$ is a standard Gaussian random vector with mean $\boldsymbol{\mu}_{\mathbf{X}}=\mathbf{0} \in \mathbb{R}^2$ and covariance matrix $\boldsymbol{\Sigma}_{\mathbf{X}}=\mathbf{I} \in \mathbb{M}_2^{S+0}(\mathbb{R})$. The purpose of this example is to predict statistical moments of eigenvalues of $\{\mathbf{K}(\mathbf{X}), \mathbf{m}\}$ by the univariate decomposition method and compare results with those obtained from mean-centred perturbation methods and the asymptotic method [15].

Figures 2(a) and (b) present surface plots of two exact eigenvalues $\lambda^{(1)}$ and $\lambda^{(2)}$ of $\{\mathbf{K}(\mathbf{X}), \mathbf{m}\}$, respectively, for $-4 \leqslant x_i \leqslant 4$; $i=1,2$, obtained by solving the matrix characteristic equation

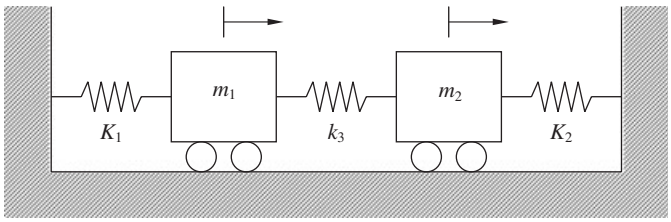

Figure 1. A two-degree-of-freedom undamped spring-mass system.

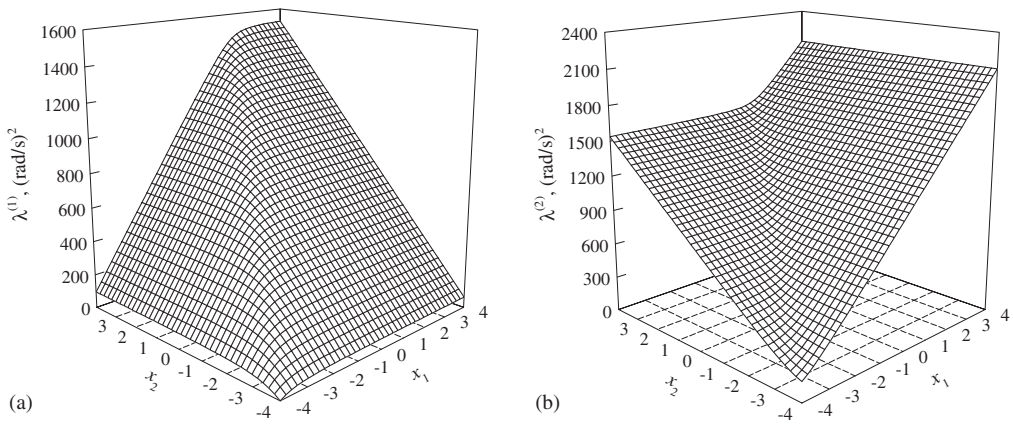

Figure 2. Exact eigenvalues for the two-degree-of-freedom system: (a) $\lambda^{(1)}$; and (b) $\lambda^{(2)}$.

(Equation (2)). Approximate eigenvalues by the univariate decomposition method (Equation (5)) and mean-centred perturbation methods were also evaluated and compared with the exact solution in terms of contour plots of $\lambda^{(1)}$ and $\lambda^{(2)}$ in Figures 3 and 4, respectively. The first- (Figures 3(c) and 4(c)) and second-order (Figures 3(d) and 4(d)) perturbation methods, which involve linear or quadratic approximations, yield contours containing significant discrepancy with the exact contours in Figures 3(a) and 4(a). In contrast, the contours generated by the univariate decomposition method (Figures 3(b) and 4(b)), which includes higher-order univariate terms, show closer agreement to the highly curved exact contours. The difference between contours by the exact method and by the univariate method is due to the absence of bivariate terms in the latter method. Nevertheless, the univariate approximation produces eigenvalue contours that agree with the exact contours better than those by either version of the perturbation method.

The proposed moment equation (Equation (12)) with $S = 1$ was employed to calculate first four moments of both eigenvalues $\Lambda^{(1)}(\mathbf{X})$ and $\Lambda^{(2)}(\mathbf{X})$ by the univariate method. Since $\mathbf{X}$ is Gaussian, a Gauss–Hermite integration rule was selected with integration orders $1 \leqslant n \leqslant 10$. Figures 5(a) and (b), respectively, depict convergence of the first moment $m_1^{(i)} \equiv \mathbb{E}[\Lambda^{(i)}(\mathbf{X})]$;

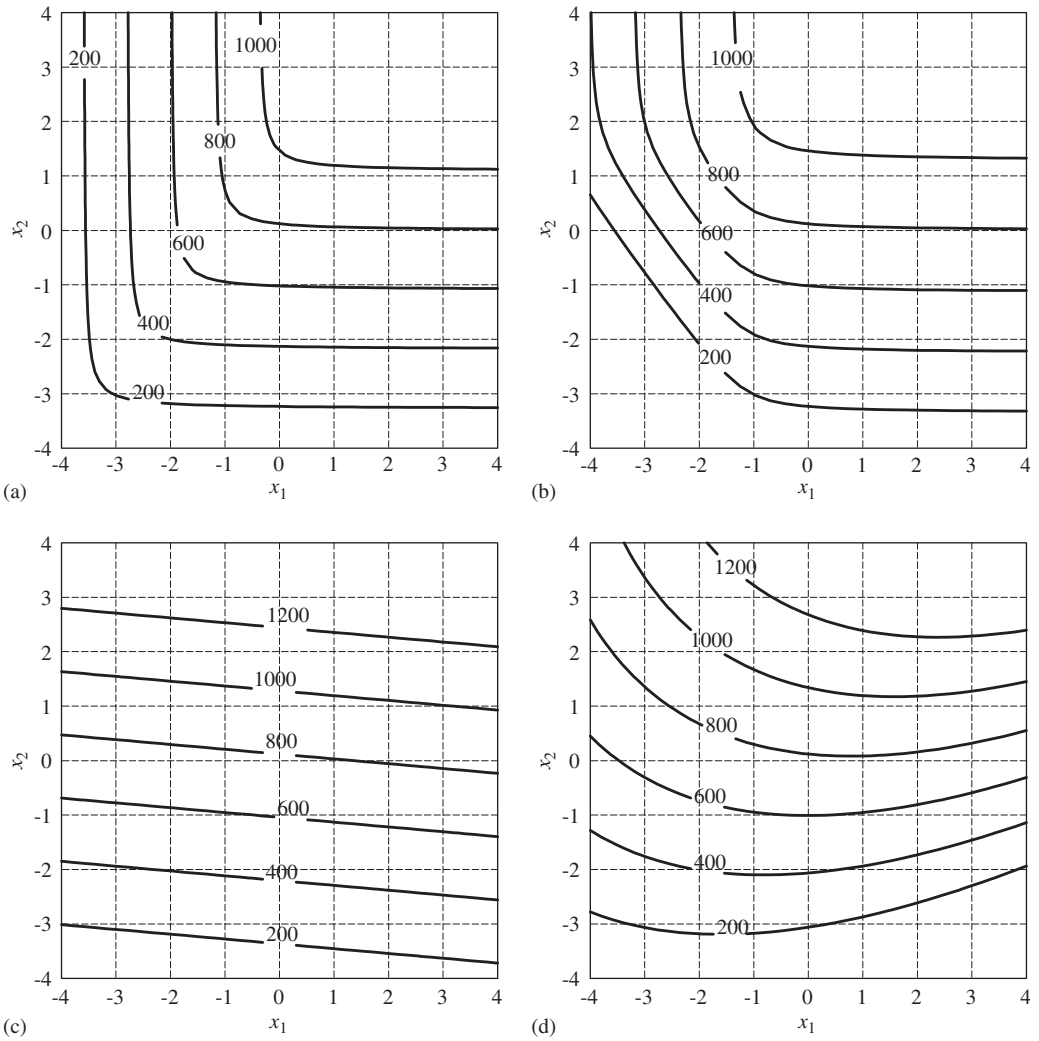

Figure 3. Contours of the first eigenvalue by various methods: (a) exact; (b) univariate decomposition; (c) first-order perturbation; and (d) second-order perturbation.

$i = 1, 2$ and the fourth moment $m_4^{(i)} \equiv \mathbb{E}[\Lambda^{(i)^4}(\mathbf{X})]$; $i = 1, 2$ with respect to n. The moments of both eigenvalues rapidly converge as n reaches 4 or 5. Hence, a value of $n = 5$ was selected for subsequent calculations in this paper.

Tables I and II list all four moments $m_l^{(i)} \equiv \mathbb{E}[\Lambda^{(i)^l}(\mathbf{X})]$; $i = 1, 2$; $l = 1, \ldots, 4$ calculated by the univariate decomposition method, first- and second-order perturbation methods, and Adhikari's asymptotic method. A direct Monte Carlo simulation involving 5000 samples of eigenvalues by repeatedly solving the matrix characteristic equation (Equation (2)) was performed to generate

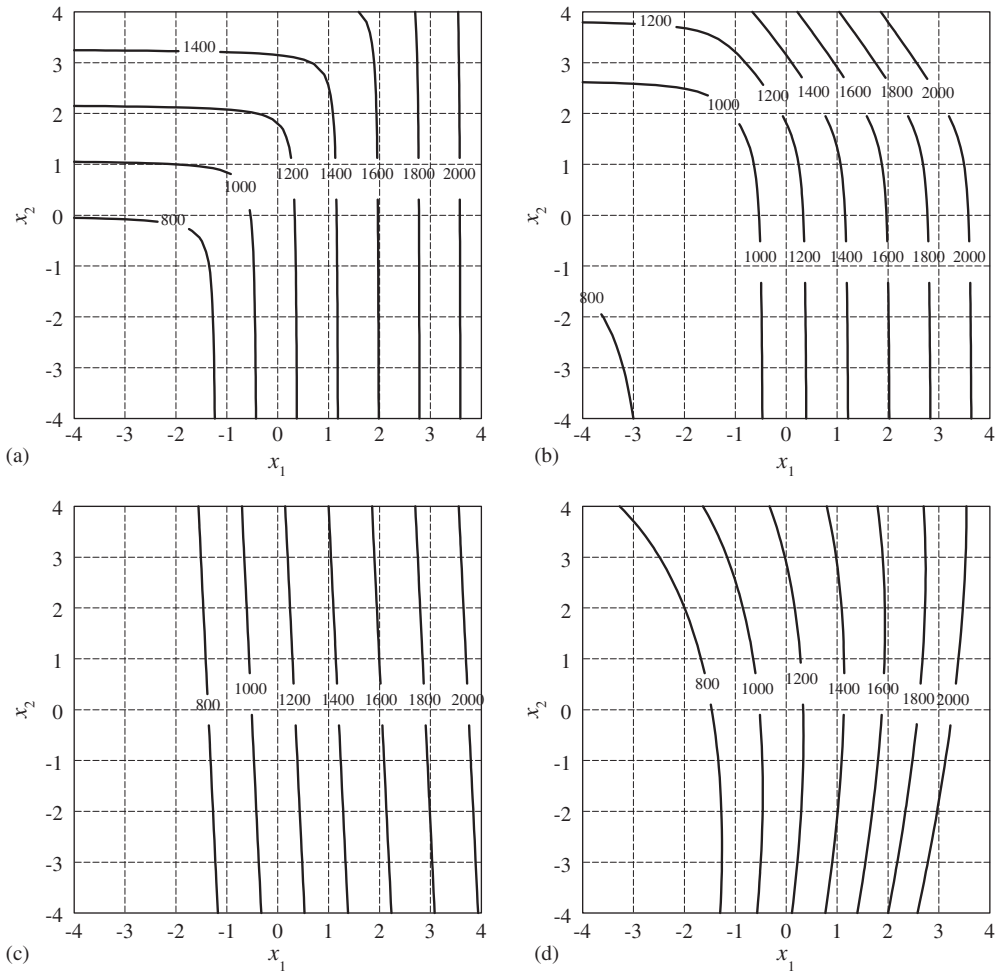

Figure 4. Contours of the second eigenvalue by various methods: (a) exact; (b) univariate decomposition; (c) first-order perturbation; and (d) second-order perturbation.

the benchmark result. The results in Tables I and II indicate that the univariate method yields the most accurate solution for this particular example. The maximum errors by the decomposition method, the first-order perturbation method, the second-order perturbation method, and the asymptotic method, measured with respect to the Monte Carlo prediction, are 3.22, 19.17, 11.17, and 5.48 per cent, respectively. It appears that the decomposition and asymptotic methods provide more accurate solutions than those by the commonly-used perturbation methods.

5.2. Example 2—a three-degree-of-freedom undamped spring-mass system

A three-degree-of-freedom undamped spring-mass system [15], shown in Figure 6, was studied to evaluate the proposed decomposition method when system eigenvalues are well-separated,

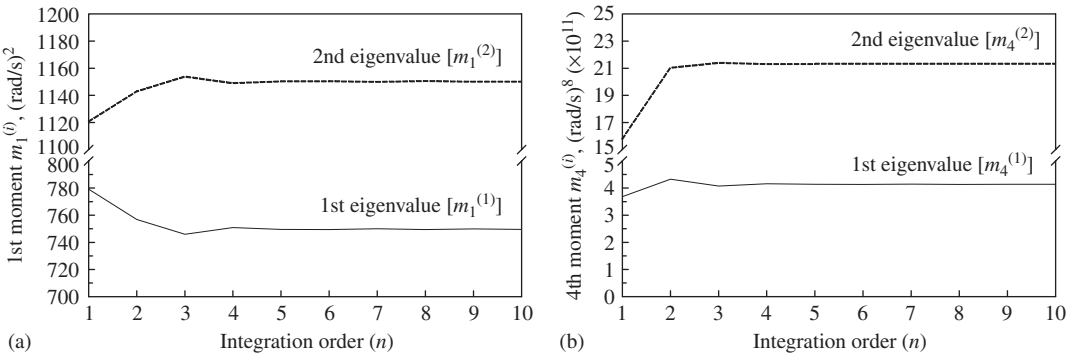

Figure 5. Convergence of moments of eigenvalues: (a) 1st moment; and (b) 4th moment.

Table I. Four moments of the first eigenvalue for the two-degree-of-freedom system.*

Moments†	Univariate decomposition method	First-order perturbation method	Second-order perturbation method	Asymptotic method [15]	Monte Carlo (5000 samples)
$m_1^{(1)}$, (rad/s)^2	7.496×10^2 (−0.52)	7.792×10^2 (−4.49)	7.631×10^2 (−2.34)	7.616×10^2 (−2.12)	7.457×10^2
$m_2^{(1)}$, (rad/s)^4	5.909×10^5 (−1.33)	6.371×10^5 (−9.25)	6.128×10^5 (−5.09)	6.028×10^5 (−3.38)	5.831×10^5
$m_3^{(1)}$, (rad/s)^6	4.858×10^8 (−2.29)	5.422×10^8 (−14.17)	5.132×10^8 (−8.06)	4.930×10^8 (−3.80)	4.749×10^8
$m_4^{(1)}$, (rad/s)^8	4.139×10^{11} (−3.22)	4.779×10^{11} (−19.17)	4.458×10^{11} (−11.17)	4.152×10^{11} (−3.53)	4.010×10^{11}

*Parenthetical values represent percentage of relative errors when compared with the Monte Carlo simulation.
†The lth moment of the first eigenvalue $m_l^{(1)} \equiv \mathbb{E}[\mathbf{\Lambda}^{(1)l}(\mathbf{X})]$; $l = 1, 2, 3,$ and 4.

closely spaced, or input uncertainties are large. The random mass and random stiffness matrices are

$$\mathbf{M}(\mathbf{X}) = \begin{bmatrix} M_1(\mathbf{X}) & 0 & 0 \\ 0 & M_2(\mathbf{X}) & 0 \\ 0 & 0 & M_3(\mathbf{X}) \end{bmatrix} \in \mathbb{M}_3^{S+0}(\mathbb{R}) \tag{24}$$

Table II. Four moments of the second eigenvalue for the two-degree-of-freedom system.*

Moments†	Univariate decomposition method	First-order perturbation method	Second-order perturbation method	Asymptotic method [15]	Monte Carlo (5000 samples)
$m_1^{(2)}$, $(\text{rad/s})^2$	1.150×10^3 (0.60)	1.121×10^3 (3.16)	1.137×10^3 (1.77)	1.133×10^3 (2.14)	1.157×10^3
$m_2^{(2)}$, $(\text{rad/s})^4$	1.369×10^6 (1.10)	1.311×10^6 (5.23)	1.348×10^6 (2.57)	1.332×10^6 (3.77)	1.384×10^6
$m_3^{(2)}$, $(\text{rad/s})^6$	1.682×10^9 (1.48)	1.597×10^9 (6.47)	1.663×10^9 (2.61)	1.625×10^9 (4.85)	1.707×10^9
$m_4^{(2)}$, $(\text{rad/s})^8$	2.133×10^{12} (1.76)	2.018×10^{12} (7.04)	2.127×10^{12} (2.02)	2.052×10^{12} (5.48)	2.171×10^{12}

*Parenthetical values represent percentage of relative errors when compared with the Monte Carlo simulation.
†The lth moment of the second eigenvalue $m_l^{(2)} \equiv \mathbb{E}[\Lambda^{(2)l}(\mathbf{X})]$; $l = 1, 2, 3,$ and 4.

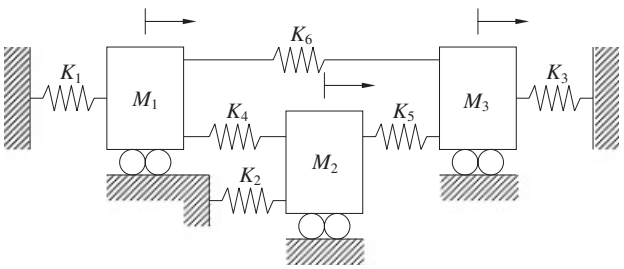

Figure 6. A three-degree-of-freedom undamped spring-mass system.

and

$$\mathbf{K}(\mathbf{X}) = \begin{bmatrix} K_1(\mathbf{X}) + K_4(\mathbf{X}) + K_6(\mathbf{X}) & -K_4(\mathbf{X}) & -K_6(\mathbf{X}) \\ -K_4(\mathbf{X}) & K_4(\mathbf{X}) + K_5(\mathbf{X}) + K_2(\mathbf{X}) & -K_5(\mathbf{X}) \\ -K_6(\mathbf{X}) & -K_5(\mathbf{X}) & K_5(\mathbf{X}) + K_3(\mathbf{X}) + K_6(\mathbf{X}) \end{bmatrix}$$
$$\in \mathbb{M}_3^{S+0}(\mathbb{R}) \tag{25}$$

respectively, where masses $M_i(\mathbf{X}) = \mu_i X_i$; $i = 1, 2, 3$ with $\mu_i = 1.0\,\text{kg}$; $i = 1, 2, 3,$ and spring stiffnesses $K_i(\mathbf{X}) = \mu_{i+3} X_{i+3}$; $i = 1, \ldots, 6$ with $\mu_{i+3} = 1.0\,\text{N/m}$; $i = 1, \ldots, 5$ and $\mu_9 = 3.0$ or $1.275\,\text{N/m}$. The input $\mathbf{X} = \{X_1, \ldots, X_9\}^{\mathrm{T}} \in \mathbb{R}^9$ is an independent lognormal random vector with mean $\boldsymbol{\mu}_{\mathbf{X}} = \mathbf{1} \in \mathbb{R}^9$ and covariance matrix $\boldsymbol{\Sigma}_{\mathbf{X}} = v^2 \mathbf{I} \in \mathbb{M}_9^{S+0}(\mathbb{R})$ with coefficient of variation $v = 0.15$ or 0.3.

Three cases involving combinations of the mean stiffness of spring 6 and the input coefficient of variation were studied: (1) Case 1: $\mu_9 = 3.0\,\mathrm{N/m}$, $v = 0.15$ (well-separated eigenvalues); (2) Case 2: $\mu_9 = 1.275\,\mathrm{N/m}$, $v = 0.15$ (closely-spaced eigenvalues); and (3) Case 3: $\mu_9 = 3.0\,\mathrm{N/m}$, $v = 0.30$ (large statistical variation of input). For all three cases a value of $n = 5$ was employed for Lagrange interpolation in the decomposition method. The sample size for the direct Monte Carlo simulation and the decomposition method was 100 000.

Case 1—well-separated eigenvalues: For Case 1, Figures 7(a)–(c) compare predicted marginal probability densities of three eigenvalues $\Lambda^{(i)}(\mathbf{X})$; $i = 1, 2, 3$ obtained by univariate and bivariate decomposition methods and the direct Monte Carlo simulation. The decomposition methods, which entail Monte Carlo analysis employing the univariate and bivariate approximations in Equations (16) and (17), permit inexpensive calculation of eigenvalues by sidestepping additional solution of the original matrix characteristic equation. Compared with the direct Monte Carlo simulation, both univariate and bivariate decomposition methods provide excellent estimates of the probability density of eigenvalues. Note that there is little statistical overlap among three eigenvalues.

Case 2—closely-spaced eigenvalues: Case 2 involves calculating probabilistic characteristics of eigenvalues that overlap, which has practical relevance to the dynamics of rotating

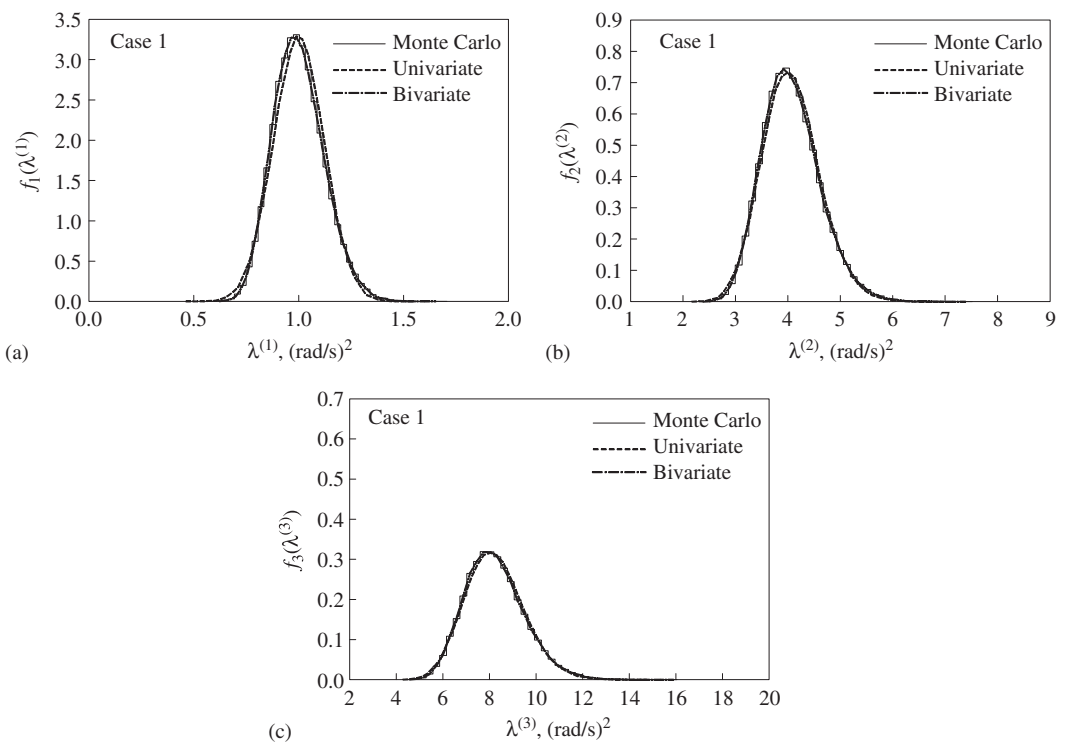

Figure 7. Probability densities of eigenvalues for Case 1: (a)$\Lambda^{(1)}$; (b) $\Lambda^{(2)}$; and (c) $\Lambda^{(3)}$.

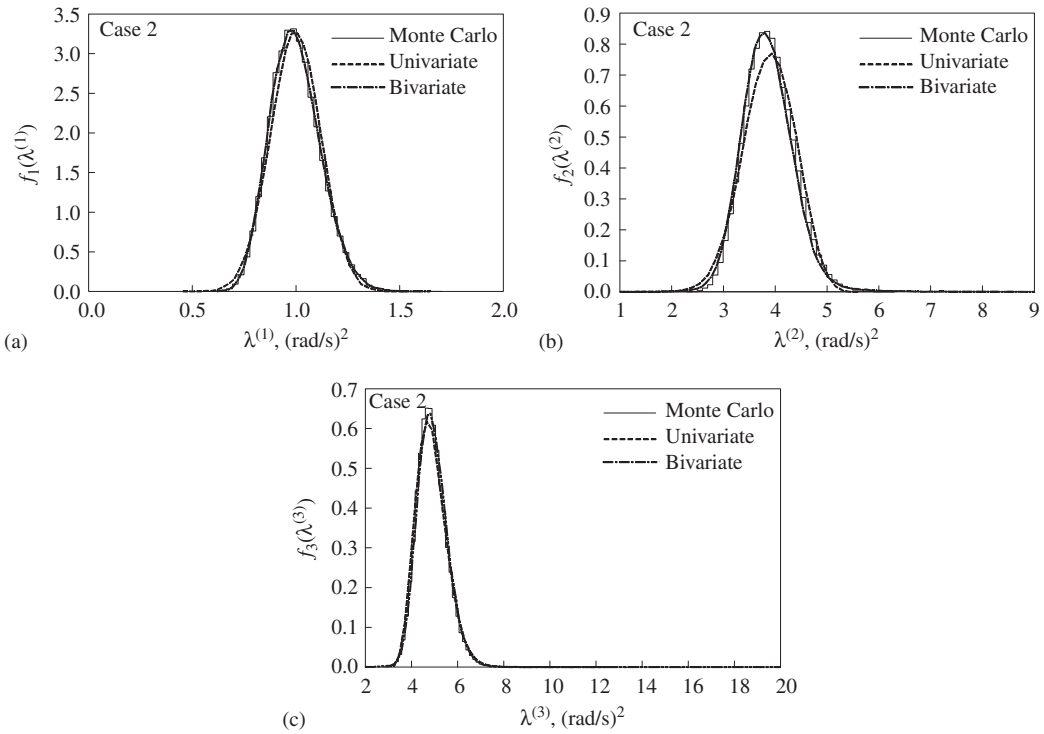

Figure 8. Probability densities of eigenvalues for Case 2: (a) $\Lambda^{(1)}$; (b) $\Lambda^{(2)}$; and (c) $\Lambda^{(3)}$.

machineries, flutter of aircraft wings, and others. Figures 8(a)–(c) present probability densities of all three eigenvalues by both versions of the decomposition method and by the direct Monte Carlo method. Indeed, there is a significant overlap between the second and the third eigenvalues with their mean values close to each other. It is well known that modal properties of such systems are parameter sensitive, leading to complicated prediction of eigenvalues [15]. From Figure 8 the probability densities obtained by the univariate method and direct Monte Carlo simulation match encouragingly well. The bivariate method yields significantly improved results, which are in close agreement with those generated by the direct Monte Carlo simulation. This improvement is possible due to hierarchical sequence of approximations in the dimensional decomposition method.

Case 3—large statistical variation of random input: The final case (Case 3) involves a large uncertainty of input, where the input coefficient of variation in Case 1 is doubled from 15 to 30 per cent. Figures 9(a)–(c) similarly compare probability densities of all three eigenvalues. It is well known that perturbation methods are not applicable for such magnitudes of input uncertainties [8–10]. However, the results in Figure 9 indicate satisfactory performance of the decomposition method even for such large uncertainties of input. It is worth noting that a larger uncertainty in input creates a larger scatter in eigenvalues, which also leads to closely-spaced modes, as depicted in Figure 9. As expected, the bivariate method is more accurate than the univariate method.

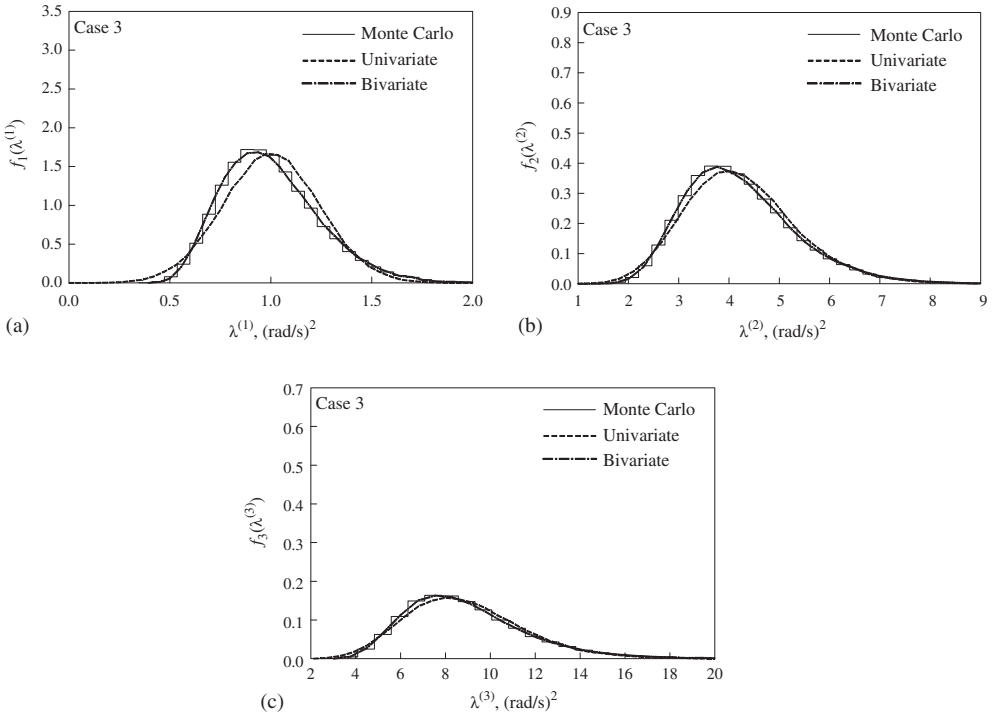

Figure 9. Probability densities of eigenvalues for Case 3: (a) $\Lambda^{(1)}$; (b) $\Lambda^{(2)}$; and (c) $\Lambda^{(3)}$.

In each of the three cases, the univariate and bivariate decomposition methods, respectively, require 37 and 613 solutions of the matrix characteristic equation, whereas 100 000 such solutions (sample size) are involved in the direct Monte Carlo simulation. However, these differences, although significant, are less meaningful given that the random matrices are only 3×3. An example where such difference has a major practical significance is demonstrated next.

5.3. Example 3—modal analysis of a fixed cantilever plate

The final example of this paper involves calculation of natural frequencies of a vibrating fixed cantilever plate with deterministic length $l = 50.8\,\text{mm}$ (2 in), deterministic width $w = 25.4\,\text{mm}$ (1 in), and random thickness t, as shown in Figure 10(a). The elastic modulus E, Poisson's ratio v, and mass density ρ are independent lognormal random variables with respective means $\mu_E = 206.8\,\text{GPa}(30 \times 10^6\,\text{psi})$, $\mu_v = 0.3$, and $\mu_\rho = 7827\,\text{kg/m}^3$ $(7.324 \times 10^{-4}\,\text{lb-s}^2/\text{in}^4)$; and respective coefficients of variations $v_E = 0.15$, $v_v = 0.05$, and $v_\rho = 0.1$. The thickness $t(\xi) = c\,\exp[\alpha(\xi)]$, which is spatially varying in the longitudinal direction (ξ), is an independent, homogeneous, lognormal random field with mean $\mu_t = 0.254\,\text{mm}$ (0.01 in), variance $\sigma_t^2 = 2.58 \times 10^{-3}\,\text{mm}^2$ $(4 \times 10^{-6}\,\text{in}^2)$, and coefficient of variation $v_t = 0.2$; where $c = \mu_t/\sqrt{1+v_t^2}$ and $\alpha(\xi)$ is a zero-mean, homogeneous, Gaussian random field with variance $\sigma_\alpha^2 = \ln(1+v_t^2)$

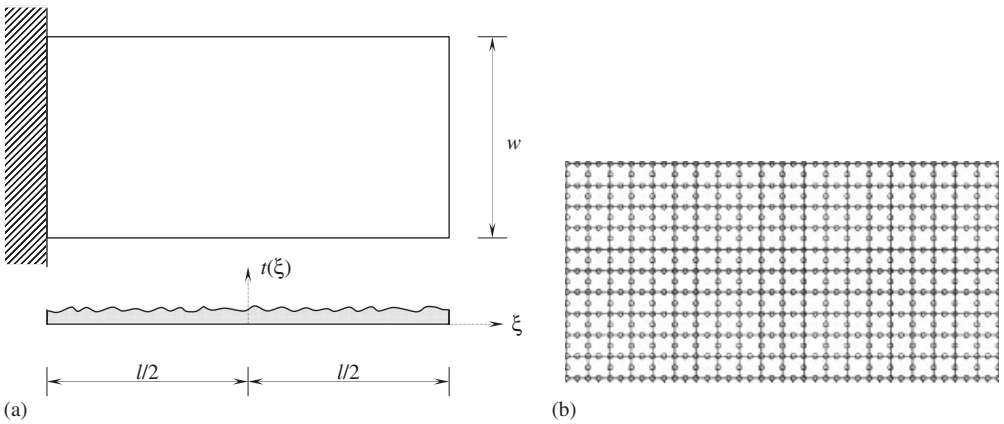

Figure 10. A fixed cantilever plate: (a) geometry; and (b) a 10×20 finite element mesh.

and covariance function $\Gamma_\alpha(\tau) \equiv \mathbb{E}[\alpha(\xi)\alpha(\xi + \tau)] = \sigma_\alpha^2 \exp(-|\tau|/0.25l)$. The Karhunen–Loève approximation was employed to discretize the random field $\alpha(\xi)$ into 12 standard Gaussian random variables [22]. Therefore, a total of 15 random variables are involved in this example.

A 10×20 finite element mesh of the plate consisting of 200 8-noded second-order shell elements (S8R5) and 661 nodes is shown in Figure 10(b). The univariate decomposition method and the direct Monte Carlo simulation using the commercial finite element code (ABAQUS) were employed for evaluating probabilistic characteristics of natural frequencies of the plate. In both methods, the calculation of the matrix characteristic equation for a given input is equivalent to performing a finite element analysis. Therefore, computational efficiency, even for this simple plate model, is a major practical requirement in solving random eigenvalue problems. For the decomposition method, a value of $n = 5$ was selected.

Figure 11 shows the first six mode shapes of the cantilever plate when the input is fixed at mean. Using samples generated from univariate approximations of eigenvalues (i.e. Equation (16)), Tables III and IV present means, standard deviations, and correlation coefficients of the six natural frequencies, which are square-root of eigenvalues. The tabular results continue to demonstrate the high accuracy of the univariate method when compared with the direct Monte Carlo simulation employing 5000 finite element analyses (samples). In contrast, only 61 finite element analyses are required by the univariate method with largest errors of 0.35, 2.4, and 1.93 per cent in calculating means, standard deviations, and correlation coefficients, respectively.

Figures 12(a) and (b) show marginal probability densities of the six natural frequencies by the univariate method and the direct Monte Carlo solution. Due to the computational expense inherent to ABAQUS analysis, the same 5000 samples generated for verifying the statistics in Tables III or IV were utilized to develop the histograms in Figure 12. However, since the decomposition method yields explicit eigenvalue approximations, an arbitrarily large sample size, e.g. 50 000 in this particular example, was selected to perform the embedded Monte Carlo analysis. Agreement between the results of the univariate decomposition method and the direct Monte Carlo simulation is excellent even when there is a significant modal overlap.

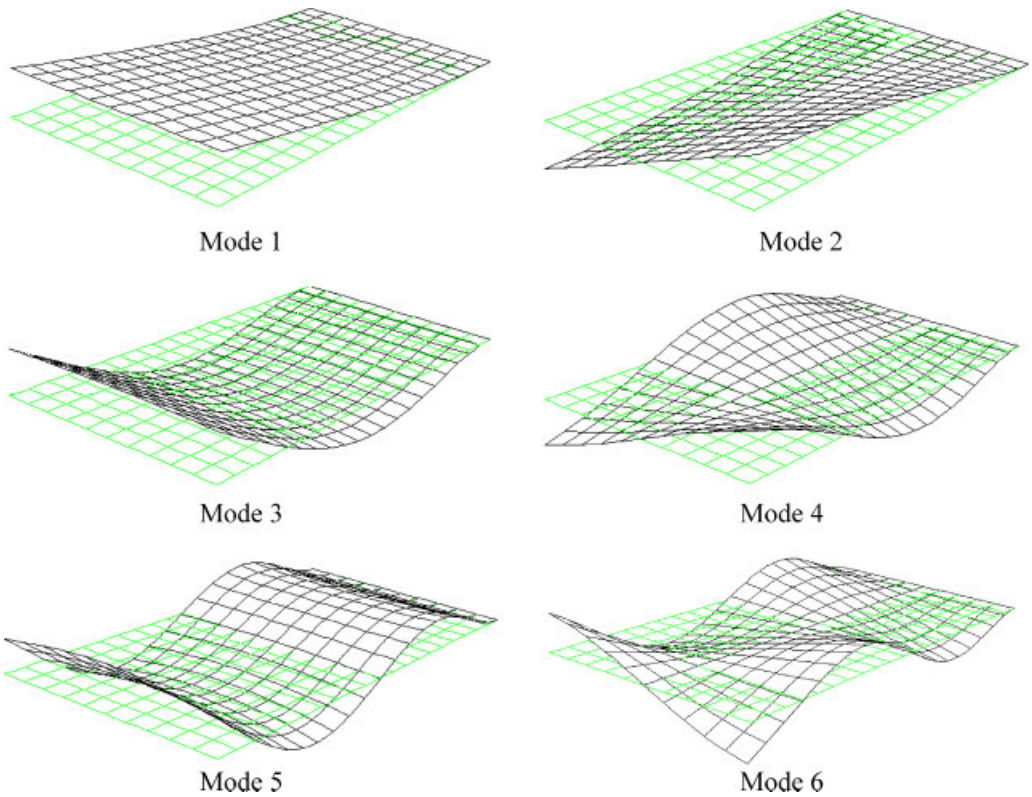

Figure 11. First six mode shapes of the fixed cantilever plate for mean input.

Table III. Means and standard deviations of first six natural frequencies for the plate.

	Mean (Hz)		Standard deviation (Hz)	
Natural frequency*	Univariate decomposition method	Monte Carlo (5000 samples)	Univariate decomposition method	Monte Carlo (5000 samples)
$\Omega^{(1)}$	81.86	81.90	19.64	19.63
$\Omega^{(2)}$	356.82	357.07	66.70	68.15
$\Omega^{(3)}$	512.88	512.99	87.31	87.54
$\Omega^{(4)}$	1173.04	1172.95	181.77	186.29
$\Omega^{(5)}$	1445.47	1446.03	230.01	232.25
$\Omega^{(6)}$	2207.99	2215.81	345.85	347.82

*The ith natural frequency $\Omega^{(i)} = \sqrt{\Lambda^{(i)}}/2\pi$; $i = 1, \ldots, 6$, where $\Lambda^{(i)}$ is the ith eigenvalue.

Table IV. Correlation properties of first six natural frequencies for the plate.

Correlation coefficient $(\rho_{ij})^*$	Univariate decomposition method	Monte Carlo (5000 samples)
ρ_{12}	0.904	0.908
ρ_{13}	0.733	0.742
ρ_{14}	0.541	0.541
ρ_{15}	0.617	0.620
ρ_{16}	0.447	0.454
ρ_{23}	0.891	0.888
ρ_{24}	0.739	0.725
ρ_{25}	0.822	0.812
ρ_{26}	0.713	0.708
ρ_{34}	0.902	0.900
ρ_{35}	0.943	0.939
ρ_{36}	0.865	0.854
ρ_{45}	0.975	0.973
ρ_{46}	0.958	0.953
ρ_{56}	0.944	0.940

$^*\rho_{ij}$ = correlation coefficient between $\Omega^{(i)}$ and $\Omega^{(j)}$; $i, j = 1, \ldots, 6;\ j > i$.

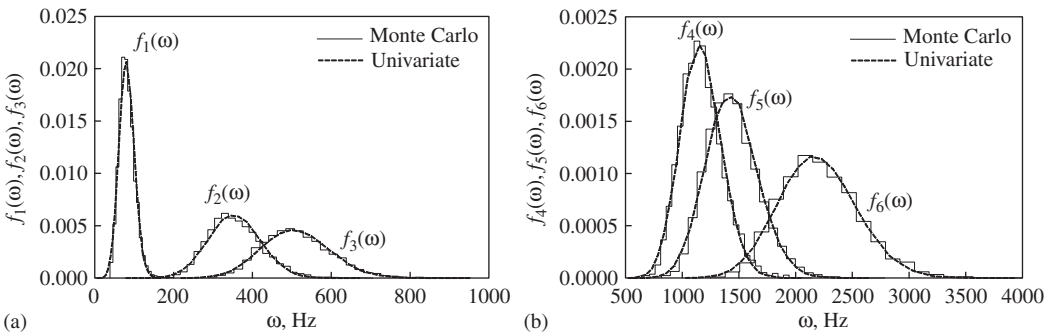

Figure 12. Probability densities of first six natural frequencies of the cantilever plate: (a) $\Omega^{(1)}$, $\Omega^{(2)}$, and $\Omega^{(3)}$; and (b) $\Omega^{(4)}$, $\Omega^{(5)}$, and $\Omega^{(6)}$.

6. CONCLUSION AND OUTLOOK

A new decomposition method was developed for probabilistic descriptors of real-valued eigenvalues of positive semi-definite random matrices. The method is based on: (1) a novel func-

tion decomposition allowing lower-variate approximations of eigenvalues; (2) lower-dimensional numerical integration for statistical moments; and (3) Lagrange interpolation facilitating efficient Monte Carlo simulation for probability density functions. The effort in finding probabilistic characteristics of eigenvalues can be viewed as performing eigenvalue analyses at selected deterministic input defined by integration points or sample points. Compared with commonly-used perturbation and recently-developed asymptotic methods, no derivatives of eigenvalues are required by the method developed. Hence, the method can be easily adapted for solving random eigenvalue problems involving third-party commercial finite-element codes. Results of numerical examples involving linear dynamics of spring-mass systems and finite element analysis of a cantilever plate indicate that the decomposition method developed provides excellent estimates of moments and probability densities of eigenvalues for various cases including closely-spaced modes and large statistical variations of input.

Although significant strides are made, further research is required on non-proportionally damped systems with complex-valued eigensolutions and on probabilistic characteristics of eigenvectors.

ACKNOWLEDGEMENTS

The author would like to acknowledge the financial support by the U.S. National Science Foundation under Grant No. DMI-0355487. The author also thanks S. Adhikari of University of Bristol for sending the results of the asymptotic method in Example 1.

REFERENCES

1. Wishart J. Generalized product moment distribution in samples. *Biometrika* 1928; **20-A**:32–52.
2. Wigner EP. On the statistical distribution of the widths and spacings of nuclear resonance levels. *Proceedings of the Cambridge Philosophical Society* 1951; **47**:790–798.
3. Wigner EP. Statistical properties of real symmetric matrices with many dimensions. *Proceedings of the 4th Canadian Mathematics Congress* 1957; 174–184.
4. Mehta ML. On the statistical properties of level spacings in nuclear spectra. *Journal of Mathematical Physics* 1960; **18**:395–419.
5. Dyson FJ. Statistical theory of the energy levels of complex systems I, II, and III. *Journal of Mathematical Physics* 1962; **3**:140–175.
6. Mehta ML. *Random Matrices* (2nd edn). Academic Press: New York, 1991.
7. Dumitriu I, Edelman A. Matrix models for beta ensembles. *Journal of Mathematical Physics* 2002; **43**: 5830–5847.
8. Boyce WE. *Probabilistic Methods in Applied Mathematics I*. Academic Press: New York, 1968.
9. Shinozuka M, Astill CJ. Random eigenvalue problems in structural analysis. *AIAA Journal* 1972; **10**(4): 456–462.
10. Zhang J, Ellingwood B. Effects of uncertain material properties on structural stability. *Journal of Structural Engineering* 1995; **121**(4):705–714.
11. Mehlhose S, Vom Scheidt J, Wunderlich R. Random eigenvalue problems for bending vibrations of beams. *Zeitschrift für Angewandte Mathematik und Mechanik* 1999; **79**:693–702.
12. Grigoriu M. A solution of the random eigenvalue problem by crossing theory. *Journal of Sound and Vibration* 1992; **158**(1):69–80.
13. Nair PB, Keane AJ. An approximate solution scheme for the algebraic random eigenvalue problem. *Journal of Sound and Vibration* 2003; **260**(1):45–65.
14. Pradlwarter HJ, Schuëller GI, Szekely GS. Random eigenvalue problems for large systems. *Computers and Structures* 2002; **80**:2415–2424.

15. Adhikari S. Statistics of eigenvalues of linear stochastic systems. *International Journal for Numerical Methods in Engineering* 2005, submitted. (Also presented at the *45th AIAA/ASME/ASCE/AHS/ASC Structures, Structural Dynamics and Materials Conference*, Palm Springs, CA, April 2004.)
16. Xu H, Rahman S. Decomposition methods for structural reliability analysis. *Probabilistic Engineering Mechanics* 2005; **20**:239–250.
17. Sobol IM. Theorems and examples on high dimensional model representations. *Reliability Engineering and System Safety* 2003; **79**:187–193.
18. Xu H, Rahman S. A generalized dimension-reduction method for multi-dimensional integration in stochastic mechanics. *International Journal for Numerical Methods in Engineering* 2004; **61**:1992–2019.
19. Rosenblatt M. Remarks on a multivariate transformation. *Annals of Mathematical Statistics* 1952; **23**:470–472.
20. IMSL Numerical Libraries. *User's Guide and Theoretical Manual*. Visual Numerics Corporate Headquarters, San Ramon, CA, 2005.
21. ABAQUS. *User's Guide and Theoretical Manual*. Version 6.5, Hibbitt, Karlsson, and Sorenson, Inc., Pawtucket, RI, 2005.
22. Ghanem R, Spanos P. *Stochastic Finite Elements*: *A Spectral Approach*. Springer: New York, 1991.

